

Crystallization-Induced Morphological Changes of a Poly(L-lactide)/Poly(oxyethylene) Diblock Copolymer from Sphere to Band via Disk: A Novel Macromolecular Self-Organization Process from Core–Shell Nanoparticles on Surface

Tomoko Fujiwara, Masatoshi Miyamoto, and Yoshiharu Kimura*

Department of Polymer Science and Engineering,
Kyoto Institute of Technology, Matsugasaki, Sakyo-ku,
Kyoto 606-8585, Japan

Received July 28, 1999

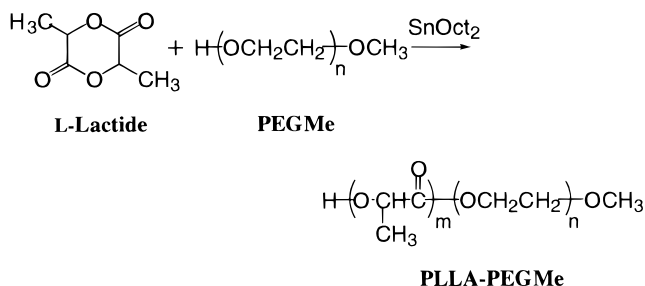
Revised Manuscript Received February 11, 2000

Introduction. Various microphase separation structures have been observed in the solid state of block copolymers.¹ Since most of the block copolymers studied thus far are made of noncrystalline segments, a repulsive force between the block segments is the main driving force in the phase separation. Another class of block copolymers, consisting of semicrystalline segments, can also form a microphase separation structure, which is quite different from that of the amorphous block copolymers because of segment crystallization in addition to microphase separation.^{2–5} However, few analyses have been conducted on the latter structure or its formation process because of its complexity.

Recently, various types of block copolymers have been prepared by a combination of poly(L-lactide) (PLLA) and poly(oxyethylene) (PEG) as the hydrophobic and hydrophilic blocks, respectively. Characteristics of these copolymers are their ease of sequence control and particle preparation as well as their wide range of applications.^{6–8} However, little research has been done on their microstructure in the solid state. Since both PLLA and PEG are crystalline, the block copolymer system affords an interesting opportunity to analyze the segment-crystallization/phase-separation processes during the macromolecular aggregation of crystalline block copolymers. In the present study, nanoparticles of a poly(L-lactide)-*block*-poly(oxyethylene) (PLLA–PEG) were prepared (Scheme 1) and developed on a substrate surface to allow the occurrence of particle destruction and aggregation until a stable morphology was constructed on the surface. The dynamic process of macromolecular dissociation, aggregation, and ordering observed during the morphological changes promotes the understanding of the mechanism of phase separation and segment crystallization of block copolymers.

Experimental Section. Poly(L-lactide)-*block*-poly(oxyethylene) monomethyl ether (PLLA–PEGMe) was synthesized by ring-opening polymerization of L-lactide (Purac Biochem, The Netherlands) in the presence of monomethoxy-terminal poly(ethylene glycol) (PEGMe: $M_n = 5000$ Da, $M_w/M_n = 1.05$, Aldrich)^{6,9} and tin octoate as the catalyst (10 mol % relative to PEGMe). PLLA–PEGMe (96% yield): $M_n = 9500$ Da, $M_w/M_n = 1.14$ (relative to polystyrene standard by GPC with CHCl_3 as eluent), PLLA/PEGMe = 52/48 (wt/wt) in a segment ratio or 40/60 (mol/mol) in a lactate/oxyethylene unit ratio.¹⁰ Its DSC curve showed two endothermic peaks at 46–57 and 140–160 °C, corresponding to the crystal

Scheme 1. Synthetic Route of a PLLA–PEGMe Copolymer



fusions of the phase-separated PEG and PLLA segments, respectively.

A suspension containing PLLA–PEGMe particles was prepared by dropwise addition of a polymer solution in tetrahydrofuran (THF) (0.25 g/5.0 mL) into water (50 mL) at 0 °C followed by sonication and evaporation of THF. The resulting aqueous suspension was filtered through a 5 μm pore filter (Fuji, FM-500). The particle concentration was then adjusted to 0.005–0.5 wt % by dilution.

Each of the suspensions prepared was cast on a freshly carved mica plate (15 \times 16 mm²) or a surface-polished Ge plate (10 \times 10 mm²) and dried up in air at 4 °C to prepare a thin film of the PLLA–PEGMe particles. Each sample thus prepared was then subjected to atomic force microscopy (AFM) conducted on a Digital Instruments Nanoscope-IIIa instrument operated in the tapping mode in air using a silicon cantilever. FT-IR spectra were measured for the samples prepared on the Ge plate on a JASCO FT/IR-5300 spectrometer.

Results and Discussion. The ¹H NMR spectrum of the copolymer suspension prepared in D₂O showed no PLLA signal despite showing a large PEG signal at $\delta = 3.6$ –3.7 ppm and a small methoxy signal at $\delta = 3.37$ ppm. This result provides strong support for the formation of core–shell particles in an aqueous medium with hydrophobic PLLA and hydrophilic PEG blocks placed in the core and shell, respectively. Dynamic light scattering (DLS; Otsuka Electronics DLS-7100) revealed that the average hydrodynamic diameter of the particles was 86–90 nm (by the cumulant method) in suspensions with concentrations of 0.005–0.5 wt %. The apparent molecular weight of the nanoparticles was determined to be 1×10^7 Da by static light scattering (SLS; Otsuka Electronics DLS-7100). From these values, the average aggregation number of the block copolymer was calculated to be ca. 1×10^3 per particle.

Each of the above suspensions was cast on a mica plate and slowly dried. Figure 1a shows a typical AFM image of the particles deposited from a concentrated (0.2 wt %) suspension. A large number of particles of a similar size agglomerate on the whole surface of the substrate. The contour of a cross section of this particle film revealed that the thickness of these particles was 5–10 nm. Therefore, the particles have a discoid shape and a dimension of 30–50 nm in diameter and 5–10 nm in thickness. Casting of those suspensions having concentrations higher than 0.1 wt % gave an identical image.

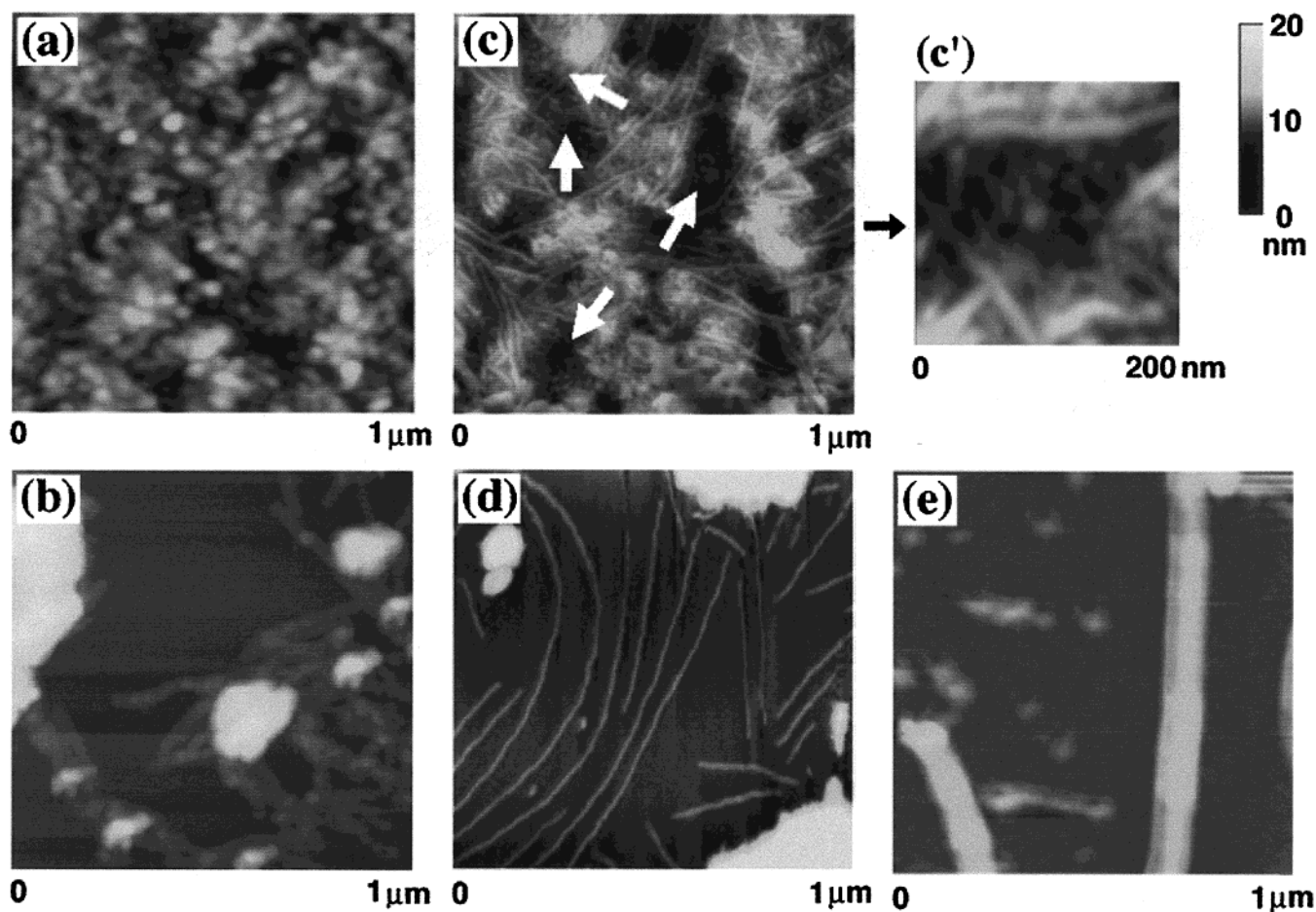


Figure 1. AFM images of the PLLA-PEG nanoparticles spread on a mica surface. Samples prepared from the 0.2 wt % suspension: (a) as-cast, (c) annealed at 60 °C for 2 h, and (c') the same as (c) recorded at higher magnification. Samples prepared from the 0.01 wt % suspension: (b) as-cast, (d) annealed at 60 °C for 2 h, and (e) kept in air for 1 week after annealing.

Figure 1b shows an AFM image of the particles deposited from a dilute suspension (0.01 wt %). It shows small particles with a diameter of 10–15 nm together with a number of large aggregates 100–500 nm in diameter. The former particles, having also a discoid shape with a thickness of ca. 2–3 nm, seem to align in a characteristic chain form. This feature suggests that the particles could not preserve their original shape on the surface if their surface density was low. Similar aggregation and collapse of the particles was also observed when a more dilute suspension (0.005 wt %) was cast. On the other hand, after the casting of a suspension with an intermediate concentration of 0.05 wt %, both the particle agglomeration state and the collapse/aggregation state were shown together in different parts of the substrate surface. On the edge of an agglomerate, several particles were found to touch the substrate surface. This observation suggests that little collapse was induced in the particles touching the substrate side of the agglomerates.

The above morphological difference should be attributed to the difference in the drying process of the suspensions. When the concentrated suspensions were loaded on the surface, they were dried up homogeneously without any water droplet forming on the surface. On the other hand, when the diluted suspensions were loaded, they were scattered in spots on the surface during drying. In this case, the deposited particles are probably subjected to biased interparticle interactions to induce collapse and aggregation.

The cast samples prepared above were annealed at 60 °C for 2 h and subjected to AFM again. Figure 1c,d shows the typical images observed after the annealing. In the sample prepared from the concentrated suspension (0.2 wt %), numerous band structures are detected together with very small fragments with a size of 5–10 nm (Figure 1c). Magnification of one region occupied by the small particles revealed that the small particles were arranged in a concentric circle with a little larger particle located in the center (Figure 1c'). This feature was observed in other regions between the bands. In the sample prepared from the dilute suspension (0.01 wt %), much longer and thicker bands were formed between the large aggregates (Figure 1d). These bands were found to grow thicker by aggregation after the sample had been kept at room temperature for a week (Figure 1e). The width of the finally obtained bands reached 100 nm, while its thickness remained 5 nm at the highest point.

The particles of a similar block copolymer of racemic poly(DL-lactide) (PDLLA: amorphous in nature) and PEG showed no band formation on the surface even after their annealing. This fact suggested that the crystallization behavior of the PLLA blocks should be closely related to the band formation. Therefore, the crystallinity was analyzed by FT-IR spectroscopy of the same particles deposited on a Ge plate. Although the surface of the Ge plate was slightly rougher than that of mica on a nanometer scale, essentially identical structures were observed for both the as-cast and

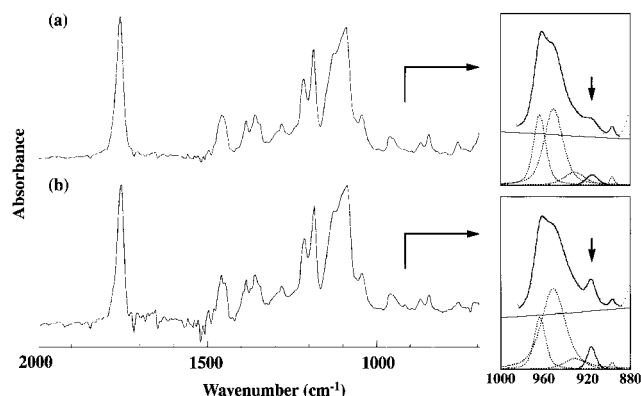


Figure 2. FT-IR spectra of the PLLA-PEG nanoparticles spread on a germanium surface: (a) as-cast and (b) annealed at 60 °C for 2 h. The peak resolving and curve fitting are shown in the enlarged spectra on the right-hand side; the bands shown by the arrows are the crystal bands of PLLA.

annealed samples. As shown in Figure 2, the helical band of PLLA was detected around 916 cm^{-1} . Its absorbance was analyzed by the curve fitting method (see the enlarged spectra in Figure 2)¹¹ and used for estimation of crystallinity of PLLA blocks.¹² The degrees of crystallinity thus determined were 0.11 and 0.24 for the (a) as-cast and (b) annealed samples, respectively. Therefore, after the heat treatment, the crystallinity of the PLLA blocks became over twice that of the original. Since the small particles involved in the annealed sample should be amorphous, the band structures themselves should have a much higher degree of crystallinity than 0.24. On the other hand, PEG-derived absorption bands were observed only in the crystal regions, suggesting a fast crystallization of the PEG blocks.

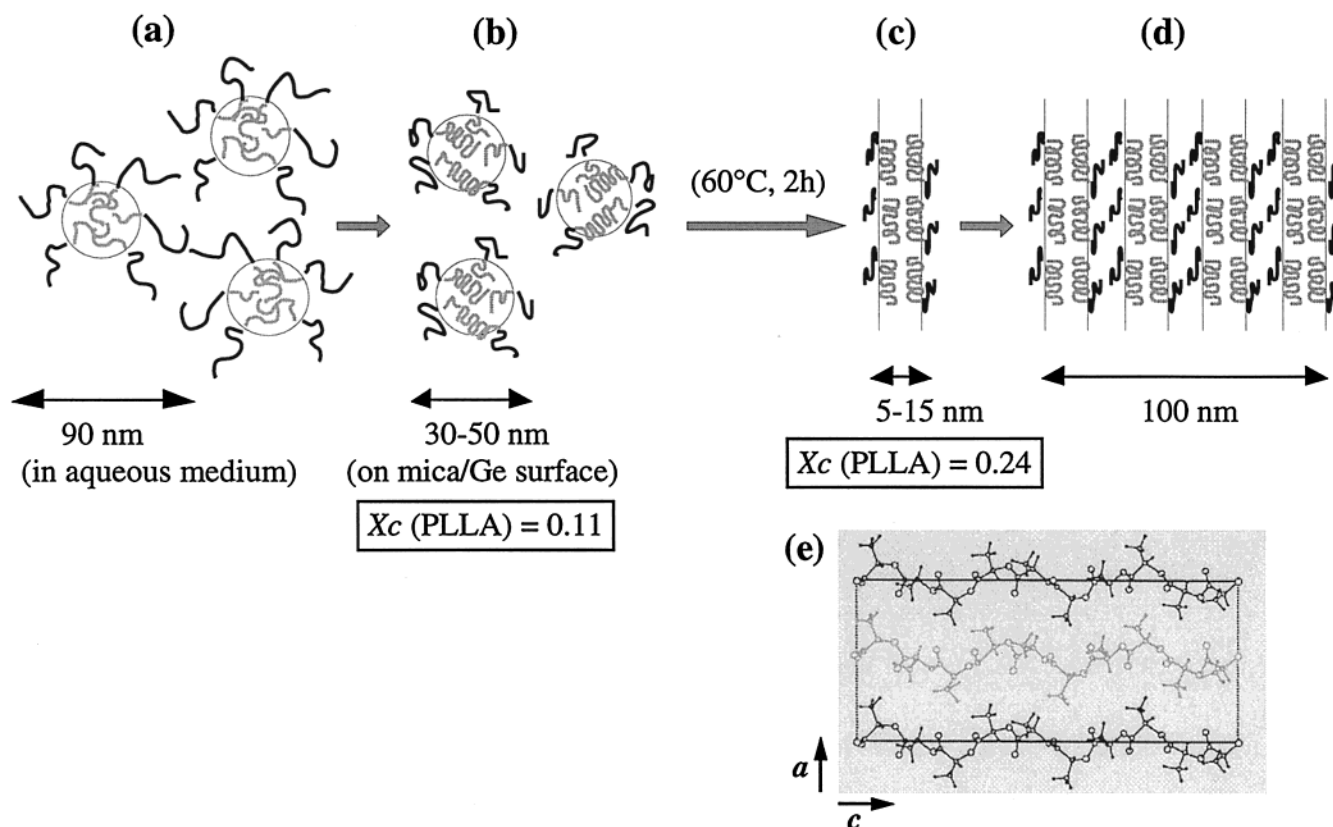


Figure 3. A schematic illustration of the morphological change of the PLLA-PEG nanoparticles: (a) in aqueous medium, (b) as-cast, (c) annealed, (d) kept in air, and (e) crystal growths of PLLA on a surface (they proceed in the direction of the a axis).

Particles of a PLLA homopolymer having a diameter of ca. 100 nm were also prepared and deposited on a mica substrate by a similar method. Their AFM observation, however, revealed that the spherical shape of the particles was maintained without structural changes even after the heat treatment. This result suggested that not only the crystallization of the PLLA blocks but also the microphase separation behavior of both blocks is responsible for the reorganization of the block copolymers.

Although the whole mechanism of the above morphological changes has not yet been clarified, the formation process of the band structures can be explained as schematized in Figure 3. The core-shell particles formed in the suspension shrink into the disks of nanometer size when they are deposited on a substrate surface in high density. The PEG blocks in the particle shell quickly crystallize in the dry state to stabilize the particles. Judging from the crystallinity of the PLLA blocks ($X = 0.11$), most of the particles contain an amorphous PLLA core, being unstable in nature, although they should contain crystal lamellae.

These disklike particles in the agglomeration state are allowed to collapse by heat treatment to form both bands and small fragments. The band formation is guided by the crystal growth of the PLLA blocks around the PLLA lamellae that have been preformed in the particles. The X-ray crystal analysis of the PLLA-PEGMe in the solid state revealed that the orthorhombic crystals of PLLA¹³ can grow in the stacking direction of the (200) or (110) plane, i.e., the a or b axis that is perpendicular to the helical macromolecular chain (c axis). Therefore, this crystal growth is induced in the thermally perturbed particles to guide the bands to extend in one direction (Figure 3c). When the helical

chains of PLLA are stacked parallel to the surface, the bandwidth is ca. 10 nm, corresponding to the block length of PLLA. This crystal dimension was really observed in the bands first formed and in the PLLA crystals primarily formed in the solid state of PLLA-PEGMe. In the following stage, these bands can further aggregate with each other to form larger bands of ca. 100 nm in width, probably through the crystal growth of the PEG segments placed around the PLLA lamellae (Figure 3d). The thickness of these bands remains 1–3 nm in order. Although the inner structure of these larger bands has not yet been clarified, we think that they should retain a phase-separation structure in which the PLLA and PEG bands are sandwiched alternately. Further studies will be needed to analyze their microstructure.

The concomitant formation of the small fragments is allowed by the collapse of the unstable particles that contain the amorphous PLLA core. The collapse happens as indicated in Figure 1c', in which several fragments are emitted around the particle center as if an explosion had occurred. This collapse is driven by the melting of the PEG crystals and the glass-to-rubber transition of the amorphous PLLA blocks ($T_g \sim 55^\circ\text{C}$). The unstable particles deposited on the surface in low concentration are directly exposed to the collapse and aggregation during the drying process. In this case, the process of lamella formation of the PLLA blocks helps the formation of the band structure as well as the alignment of the small fragments in line (Figure 1b) despite the premature state of the crystalline lamellae.

References and Notes

- (1) Araki, T.; Tran-Cong, Q.; Shibayama, M. *Structure and Properties of Multiphase Polymeric Materials*; Marcel Dekker Inc.: New York, 1998.
- (2) Wunderlich, B. *Macromolecular Physics*; Academic Press: New York, 1973; Vol. 1.
- (3) Rangarajan, P.; Register, R. A.; Adamson, D. H.; Fetters, L. J.; Bras, W.; Naylor, S.; Ryan, A. J. *Macromolecules* **1995**, *28*, 1422.
- (4) Ryan, A. J.; Hamley, I. W.; Bras, W.; Bates, F. S. *Macromolecules* **1995**, *35*, 3479.
- (5) Nojima, S.; Hashizume, K.; Rohadi, A.; Sasaki, S. *Polymer* **1997**, *38*, 2711.
- (6) Gref, R.; Minamitake, Y.; Peracchia, M. T.; Trubetskoy, V.; Torchilin, V.; Langer, R. *Science* **1994**, *263*, 1600.
- (7) Hagan, S. A.; Coombes, A. G. A.; Garnett, M. C.; Dunn, S. E.; Davies, M. C.; Illum, L.; Davis, S. S. *Langmuir* **1996**, *12*, 2153.
- (8) Jeong, B.; Bae, Y. H.; Lee, D. S.; Kim, S. W. *Nature* **1997**, *388*, 860.
- (9) Lee, C. W.; Kimura, Y. *Bull. Chem. Soc. Jpn.* **1996**, *69*, 1787.
- (10) ^1H NMR (CDCl_3): δ 1.56–1.6 (d, CH_3 for PLLA), 3.37 (s, OCH_3 for PEGMe), 3.6–3.7 (m, $\text{CH}_2\text{CH}_2\text{O}$ for PEG), 4.3–4.4 (m, COOCH_2 for the oxymethylene connecting with the PLLA sequence), and 5.1–5.2 (q, CH for PLLA).
- (11) Kister, G.; Cassanas, G.; Vert, M.; Pauvert, B.; Terol, A. *J. Raman Spectrosc.* **1995**, *26*, 307.
- (12) Wide-angle X-ray scattering (WAXS) of a PLLA sample showed two reflections at $2\theta = 17^\circ$ and 19° due to the α -crystal cells.¹³ The degree of crystallinity (X) of the sample was estimated according to the literature method.¹⁴ The relative IR absorbance [A_{916}/A_{1756}] in reference to the carbonyl band around 1756 cm^{-1} that was independent of crystallinity of PLLA can be well related with the crystallinity (X) of the PLLA blocks by such an equation as $X = 23[A_{916}/A_{1756}]$.
- (13) Kobayashi, J.; Asahi, T.; Ichiki, M.; Okikawa, A.; Suzuki, H.; Watanabe, T.; Fukuda, E.; Shikunami, Y. *J. Appl. Phys.* **1995**, *77*, 2957.
- (14) Ohkoshi, Y.; Shirai, H.; Gotoh, Y.; Nagura, M. *Sen'i Gakkaishi* **1999**, *55*, 21.

MA991253J